Molecular dynamics study of chemically induced phase transformation

A. M. Krivtsov
akrivtsov@bk.ru

Abstract

A molecular dynamics model for the phase transformation induced by chemical reaction (oxidation) is presented. The material properties such as density, stiffness and strength are being changed due to the oxidation. In contrast with the previous works [2] the oxidation is considered not only on the material surface, but also inside the material at the phase boundaries. A square specimen with periodic boundaries and central circular hole is considered, which is equivalent to an infinite material with a periodic set of holes. Oxidation starting from the inner surface of the hole and resulting in the hole closure is investigated. Influence of the reaction probability on the velocity of the chemical reaction front, velocity of the hole surface, thermal motion, and defects density are analyzed. In addition oxidation starting from the outer surface of a circular and square specimens is considered.

1 Introduction

The molecular dynamics (MD) models for investigation of mechanical processes in solids become more and more popular in the last decades. However relatively low number of papers are devoted to MD modelling of interaction between chemical and mechanical processes in solids. This paper is making attempt to set up an investigation in this area, considering processes close to the processes taking place in microscopic silicon specimens subjected to mechanical loading and oxidation [1]. The results of such processes can be applied for description of fracture and ware in microelectromechanical systems.

In the previous paper [2] a molecular dynamics model for fracture accompanied by chemical reaction was suggested; crack initiation and development in specimens subjected to an uniaxial loading was considered. The oxidation of the initial and new specimen surfaces during the fracture process were taken into account. It was postulated that the material properties such as density, stiffness and strength were changing due to the oxidation. Influence of the chemical reaction (oxidation) on the fracture scenario was investigated. Fracture process for the specimens of different shape, with and without predefined defects was studied.

In the previous work [2] the chemical reaction was applied only for the boundary particles (the particles having less nearest neighbors then in the perfect crystal). In this case only a surface oxidation takes place. The material is covered by a thin film of oxide, which does not penetrate inside the material. Such situation is realized, for example, for aluminium, for which the oxide coverage preserves the rest of the material from the further oxidation. However, for some other materials, such as silicon, the oxide has porous structure, which allows penetration of oxygen. In such cases the width of the oxide film grows with time. This effect is especially important at micro- and nanoscale, where the relative speed of oxidation is much higher then at the macroscale. In particular, for MEMS made from silicon the oxidation process is essential, since the mechanical properties of the silicon dioxide differs essentially from those of the pure silicon [1]. Investigation of such processes is the main subject of the current paper.

2 Simulation technique

The simulation procedure applied in this work is similar to that used at the previous stage of the project. The basic molecular dynamics technique used below is described in [3, 4], in more details it is described in [5, 6]. The material is represented by a set of particles interacting through a pair potential $\Pi(r)$. The equations of particle motion have the form

$$m\ddot{\underline{r}}_k = \sum_{n=1}^{N} \frac{f(|r_k - r_n|)}{|r_k - r_n|} (\underline{r}_k - \underline{r}_n) - B\dot{\underline{r}}_k, \tag{1}$$

where $\underline{r}_k$ is the radius vector of the k-th particle, m is the particle mass, N is the total number of particles, $f(r) \stackrel{\text{def}}{=} -\Pi'(r)$ is the interparticle interaction force, B is a dissipation coefficient. We use the following notation: a is the equilibrium distance between two particles ($f(a) = 0$), $D \stackrel{\text{def}}{=} |\Pi(a)|$ is the bond energy, C is the stiffness of the interatomic bond in equilibrium, and T_0 is the oscillation period of the mass m under the action of a linear force with stiffness C

$$C \stackrel{\text{def}}{=} \Pi''(a) \equiv -f'(a), \qquad T_0 = 2\pi\sqrt{m/C}. \tag{2}$$

We will use the quantities a and T_0 as microscopic distance and time scales. For a particle of mass m that is in equilibrium in the potential field $\Pi(r)$ its minimum velocity to reach infinity is $v_d = \sqrt{2D/m}$ — so called dissociation velocity. The velocity of long waves of small amplitude in 1D chain is $v_0 = a\sqrt{C/m}$. We will use v_d and v_0 as a velocity scale units. To measure the level of thermal motion in material the velocities deviation Δv (mean-square value of random thermal velocities, further Δv is referred as heat velocity) will be used. When Δv approaches dissociation velocity v_d then the thermal motion break the internal bonds in the material resulting in its melting. The last term in equation (1) is used to describe energy losses of different kind, such as radiation, internal friction, and heat conductivity. The unit for the friction coefficient is

$$B_0 \stackrel{\text{def}}{=} 2\sqrt{mC} \tag{3}$$

that is the critical value of friction for a mass m on a spring C.

Let us consider the classical Lennard–Jones potential:

$$\Pi_{LJ}(r) = D\left[\left(\frac{a}{r}\right)^{12} - 2\left(\frac{a}{r}\right)^{6}\right], \tag{4}$$

where D and a are the bond energy and the equilibrium interatomic distances, introduced earlier. The corresponding interaction force $f(r) = -\Pi'(r)$ has the form

$$f_{LJ}(r) = Q\left[\left(\frac{a}{r}\right)^{13} - \left(\frac{a}{r}\right)^{7}\right], \qquad Q \stackrel{\text{def}}{=} \frac{12D}{a}, \tag{5}$$

where Q is the interparticle force magnitude. In the case of the Lennard–Jones potential, the stiffness C and the bond energy D obey the relation $C = 72D/a^2$; the force (5) reaches its minimum value (the bond strength) at $r = b = \sqrt[6]{13/7}$, where b is the break distance. The corresponding break deformation of the Lennard–Jones bond is $\varepsilon_* = b - a \approx 0.109$. The Lennard–Jones potential is the simplest potential that allows one to take into account the general properties of interatomic interaction: repulsion of particles that approach each other, attraction of particles moving away from each other, and the absence of interaction at large distances between them. For calculations the shortened Lennard–Jones interaction will be used, given by formula

$$f(r) = \begin{cases} f_{LJ}(r), & 0 < r \le b, \\ k(r) f_{LJ}(r), & b < r \le a_{\text{cut}}; \end{cases} \tag{6}$$

where b is break distance for Lennard-Jones potential, a_{cut} is cut-off distance (for $r > a_{\text{cut}}$ the interaction vanishes). The coefficient $k(r)$ is the shape function

$$k(r) = \left[1 - \left(\frac{r^2 - b^2}{a_{\text{cut}}^2 - b^2}\right)^2\right]^2. \tag{7}$$

The cut-off distance will be set as $a_{\text{cut}} = 1.4a$, in this case only the first neighbors are interacting for the close-packed structures. For the general study of the fracture process this simplified potential is sufficient. If necessary the obtained results can be extended to more complex potentials describing the properties of materials more exactly.

For simulation a two-dimensional material will be used, where particles are packed to form an ideal 2D close-packed (triangular) crystal lattice. This is simplified lattice, however its symmetry is same as the symmetry of [111] surfaces of 3D crystal lattices, such as FCC and diamond (the last one is the lattice of silicon crystals). For the computations periodic boundary conditions are applied at all boundaries. The vertical lattice orientation is used for all computations (this means that rhombic elementary cells of the lattice are directed vertically).

The typical values of the mentioned computation parameters are given in Table 11.

3 Chemical reaction modelling

For the oxidation simulation the following model is suggested. The properties of particles adjusting to the surfaces are changed mimicking the difference between the original material and its oxide: size of the particles became slightly bigger, the elastic and strength properties became substantially lower then for the initial particles. This change take place immediately and involves the particles surrounding the original surfaces of the specimen, as well as the particles laying near the new surfaces provided by the fracture and crack development. Since the size of the particles increases, this can provide separation of the pieces of material — the oxidization induced fracture. In this case fracture and chemical reaction can stimulate each other resulting in a self-generating process. Although mainly we will be studying situations when the chemical reaction front propagates due to the oxygen transfer through the oxide.

In the case of oxidation it is postulated that the properties of the particles are being changed. The diameter and force magnitude for the oxidized particles will be denoted as $\tilde{a}$ and $\tilde{Q}$. The vector of the interaction force between two original particles can be represented as following

$$\underline{f} = \Phi(r^2)\underline{r}\,, \qquad \Phi(r^2) \stackrel{\text{def}}{=} f(r)/r. \tag{8}$$

When one or both of the interacting particles are oxidized then the interaction law takes the form

$$\underline{f} = \Phi\left(\lambda(r^2 - \overline{a}^2) + a^2\right)\underline{r}\,, \qquad \lambda \stackrel{\text{def}}{=} a^2/\overline{a}^2, \tag{9}$$

where function Φ is calculated using average values for the particle diameter and force magnitude:

$$\overline{a} \stackrel{\text{def}}{=} (a_1 + a_2)/2\,, \qquad \overline{Q} \stackrel{\text{def}}{=} (Q_1 + Q_2)/2; \tag{10}$$

indexes 1 and 2 correspond to the first and the second interacting particle. This interaction law preserves the width of the potential well independently of the particles sizes.

For the chemical reaction initiation two following mechanisms are used.

Surface oxidation. The particle changes its status from original to the oxidized one if in the distance a_c it has less then n_c neighbors, where n_c is the neighbors count for the perfect crystal (in the case of triangular lattice $n_c = 6$).

Internal oxidation. The particle changes its status from original to the oxidized one if it has at least one oxidized neighbor.

The first mechanism of the oxidation modelling was used in [2]. It gives only the surface oxidation, therefore the chemical reaction can penetrate inside the material only in the case of fracture. The second mechanism is introduced in the current paper and it simulates the oxidation due to the oxygen transfer through the oxidized zone. In paper [2] only the surface oxidation was considered, therefore the oxidation was applied immediately, at every computation step. However if the second mechanism would be used in the same manner it would produce a very fast motion of the chemical reaction front. The corresponding velocity of the reaction front in 1D chain can be calculated as

$$v_c = \frac{a}{\Delta t} \quad \Rightarrow \quad \frac{v_c}{v_0} = \frac{1}{2\pi}\frac{T_0}{\Delta t}. \tag{11}$$

To alternate the front propagation velocity the chemical reaction is applied with probability $0 \leq r_p \leq 1$. This means that at every check a random number $r \in [0, 1]$ is generated and reaction takes place only if $r < r_p$. For 1D chain such algorithm would give for the front velocity v_f

$$v_f = r_p v_c. \tag{12}$$

In 2D crystal with close packed triangular lattice relation (12) holds only for r_p close to 1, in other cases it becomes $2 \div 3$ times grater — see Table 10.

r_p	1	0.1	0.01	0.001	0.0002
$v_f/(r_p v_c)$	0.94	2.49	2.83	2.95	3.02

Table 10: Relation between reaction probability r_p and velocity of the reaction front v_f.

The typical values of the mentioned computation parameters are given in Table 11.

4 Oxidation of material with circular holes

To investigate the oxidation process a square specimen with a central circular hole is considered — see Fig. 1a. The boundary conditions are periodical, so the situation is equivalent to an infinite

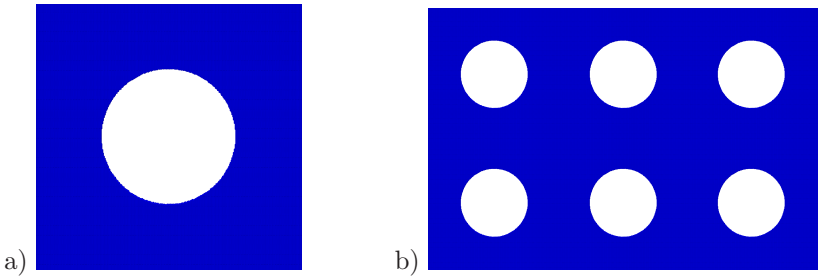

Figure 1: a) The specimen with a circular hole; b) periodic material combined from the specimens.

material with periodically located holes, arranged in a square lattice — Fig. 1b. The hole diameter is taken to be a half of the specimen width, that means that in the periodical material the hole diameter is equal to the width of the material bridge between the holes. In this case the hole volume V_{hole} is slightly less then 20% of the specimen volume V_{spec}:

$$\frac{V_{\text{hole}}}{V_{\text{spec}}} = \frac{\pi R^2}{L^2} = \frac{\pi^2}{16} \approx 0,19635, \tag{13}$$

where R is radius of the hole, L is width of the specimen. The chemical inflation $\tilde{a}/a = 1.2$ will be used in the computer experiments. Therefore if all the material would be oxidized, then enough of additional material volume would be produced to fill the hole. The considered value of the chemical inflation is higher then in the case of silicon oxidation, where $\tilde{a}/a = 1.1$. The higher value is used to have better pronounced results, most of the qualitative conclusions from this investigation can be used for the case of lower value of the chemical inflation.

The computational parameters are listed in Table 11. All the parameters are kept constant except of the last two. The main task would be to study the influence of the reaction probability r_p on the oxidation process. The value of the reaction probability determines the speed of the chemical reaction and consequently, the speed of the chemical front propagation. Therefore, the lower is r_p, the longer calculation time $t_{\max}$ is required (the second parameter being varied in Table 11).

Results of the computer experiment for the value of the reaction probability $r_p = 0.01$ are shown in Fig. 2, and zoom-up of Fig. 2a is presented in Fig. 3. Blue color in the figure represents the original material, cyan color represents the oxide, dark cyan outlines the particles of boundaries and defects (the particles having less then 6 neighbors). The figure shows, that oxidation zone

Parameter	Symbol	Value
Number of particles	N	80 311
Cut-off radius	a_{cut}	$1.4\,a$
Initial velocity deviation	Δv	$0.005\,v_d$
Dissipation coefficient	B	$0.026\,B_0$
Integration step	Δt	$0.02\,T_0$
Chemical inflation	$\tilde{a}/a$	1.2
Chemical strengthening	$\tilde{Q}/Q$	1/3
Neighborhood radius	a_c	$1.2\,a$
Neighbor count	n_c	6
Relative hole diameter	$2R/L$	0.5
Lattice orientation		vertical
Boundary conditions		periodic
Reaction probability	r_p	$0.0002 \div 1$
Calculation time	$t_{\max}$	$400 \div 5000\,T_0$

Table 11: Computation parameters.

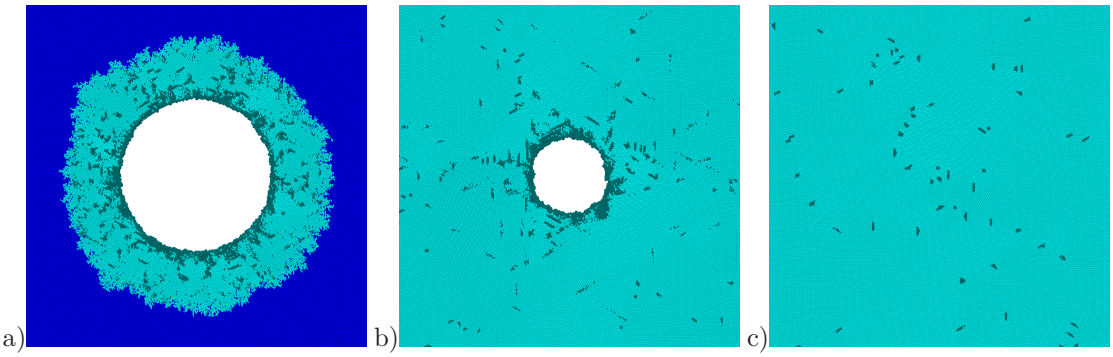

Figure 2: Sequential stages of the oxidation process: a) $t = 30\,T_0$, b) $t = 200\,T_0$, c) $t = 600\,T_0$.

starts from the hole surface, it grows and fills all the specimen, the hole size decreases and finally the hole completely disappears. No sign of the hole is seen in the last frame, only some defects are more or less uniformly distributed across the specimen. The zoom-up of the process of the hole disappearance is shown in Fig. 4. Finally the hole transforms to a group of dislocations, which then move to other parts of the specimen.

Time dependencies of the front radius R_f, and the hole radius R_h for the high and low reaction probability r_p are shown in Fig. 5. The values of the radii are calculated by measuring the volume occupied by the oxide and the volume of the hole, using the assumption that the mentioned areas are circular. For the high reaction probability the chemical front velocity is higher then the hole surface velocity. Therefore in this case all the material is oxidized earlier then the hole disappears. On contrary, for the low reaction probability the hole disappears first, and only after that the remains of the original material are oxidized. This difference can be observed in Fig. 6, where the specimens at the moment when the reaction front reaches the specimen boundaries are shown for different values of the reaction probability. The radii of the oxidized zone for all specimens in Fig. 6 are approximately the same, but the radii of the holes are different: the slower moves the reaction front, the more time the material has to decrease the hole. The oxidized zone is not circular only for $r_p = 1$ — the anisotropy of the lattice takes effect; for the smaller considered values of r_p (0.1 and lower) no anisotropy of the chemical front propagation can be noticed.

The time dependence of the hole surface velocity for the high and low r_p are shown in Fig. 7. Blue curve shows the original plot, black stands for the plot averaged over 5 nearest moments of time. According to the graphs the velocity of the hole surface is not constant, it decreases with time for the high values of r_p and increases with time for the low values. This effect is due to the differences in the front velocity. In the first case for the most of time the whole specimen is

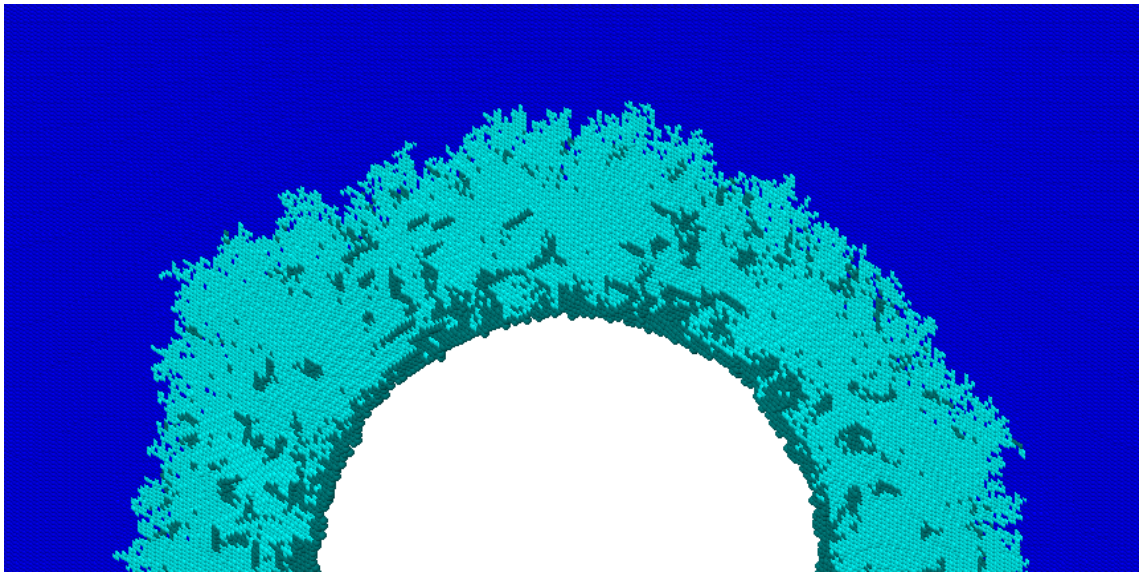

Figure 3: Half of the specimen, $t = 30\,T_0$.

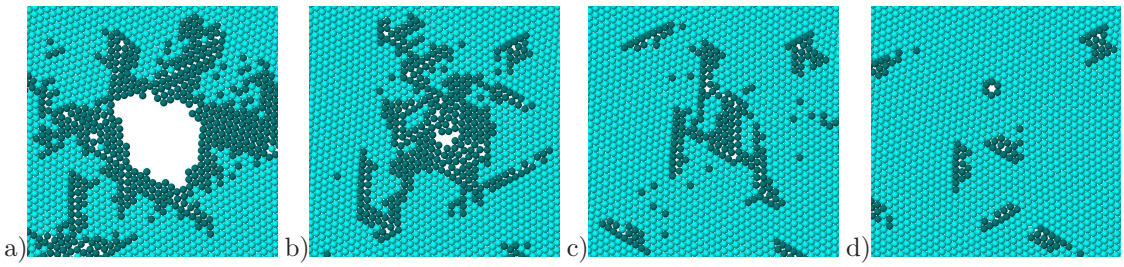

Figure 4: Zoom-up of the hole disappearance: a) $t = 430\,T_0$, b) $t = 480\,T_0$, c) $t = 490\,T_0$, d) $t = 500\,T_0$.

oxidized and the hole closure process is highly dynamical. In the second case the hole closure can be treated as quasistatical process, which follows the slow propagation of the reaction front.

This difference is also illustrated by Fig. 8, where the heat velocity Δv is shown as a function of time for high and low values of r_p. Let us note that the material temperature is proportional $(\Delta v)^2$. The heat velocity is shown in the units of dissociation velocity[1] v_d. In this case Δv approaching unity $(1v_d)$ corresponds to the material melting. From the figures it follows that for the high values of r_p the heating of material is much higher, then for the lower r_p, that is additional proof that the in the first case the process is highly dynamical. In these graphs the defects density is also shown, which is calculated as a ratio of the material volume, occupied by defects to the whole volume of the specimen. The time dependence of the defects density in these two cases is different. For the high r_p the defects density has a sharp maximum at the very beginning, when the oxidation starts, and then it slowly decreases. For the low r_p the defects density demonstrates graph with a well pronounced maximum at intermediate values of time. The explanation of this difference is that the defects are mainly produced by the propagation of the chemical reaction front. If the front propagates slower then the maximum is shifted to the later times. However, according to the graphs, the maximum value in this case is higher — this is an unexpected result requiring some explanation.

The summarizing graphs showing relations of the mentioned above quantities on the reaction probability r_p are presented in Fig. 9. From the graphs in Fig. 9a it follows that the velocities of the reaction front and the hole surface differ a lot for the high values of r_p. As the reaction probability

[1]Here and below for the sake of simplicity the dissociation velocity is calculated as $v_d = \sqrt{2D/m}$, where D is the bond energy for the classical Lennard-Jones potential (4), but not for the shortened Lennard-Jones interaction (6), which is actually used in the computations.

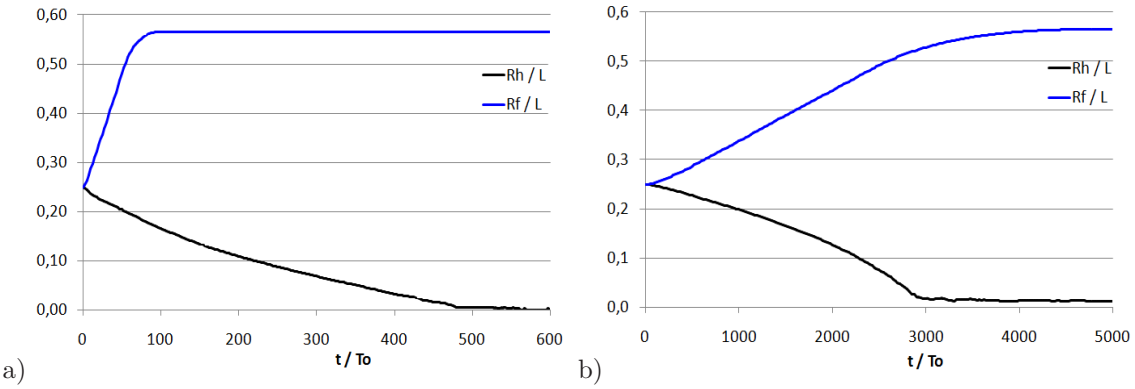

Figure 5: Time dependenceies of the front radius R_f and the hole radius R_h for two values of the reaction probability: a) $r_p = 0.01$, b) $r_p = 0.0002$.

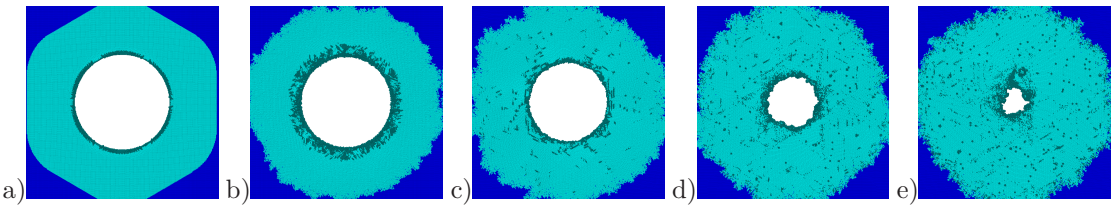

Figure 6: Specimens at the moment when the reaction front reaches their boundaries: a) $r_p = 1$, $t = 1.6\,T_0$; b) $r_p = 0.1$, $t = 6\,T_0$, c) $r_p = 0.001$, $t = 55\,T_0$, d) $r_p = 0.0001$, $t = 540\,T_0$, e) $r_p = 0.00002$, $t = 2600\,T_0$.

decreases then these velocities became closer, demonstrating a quasistatic process. Logarithm scales are used along the both axes. The velocities are shown in the units of v_0 — the sound velocity in the material. For r_p equal to 0.01 or greater the front velocity is even higher then the speed of sound. The hole surface velocity obviously is less then the sound speed, and therefore a great difference between these two velocities is observed for the higher values of r_p. For the lower r_p both velocities became proportional to each other and to the velocity $r_p v_c$ of the reaction front in 1D, which is shown in Fig. 9a by a dashed line.

The heat velocity, according to Fig. 9b is decreasing with decreasing of the reaction probability. This is an expected result, but strange behavior is observed for higher r_p, where the maximum is observed for $r_p = 0.1$. The defects density, also shown in this graph, increases with r_p decrease, and this fact is not explained yet.

Actually the most realistic situation corresponds to the quasistatic processes at the lower values

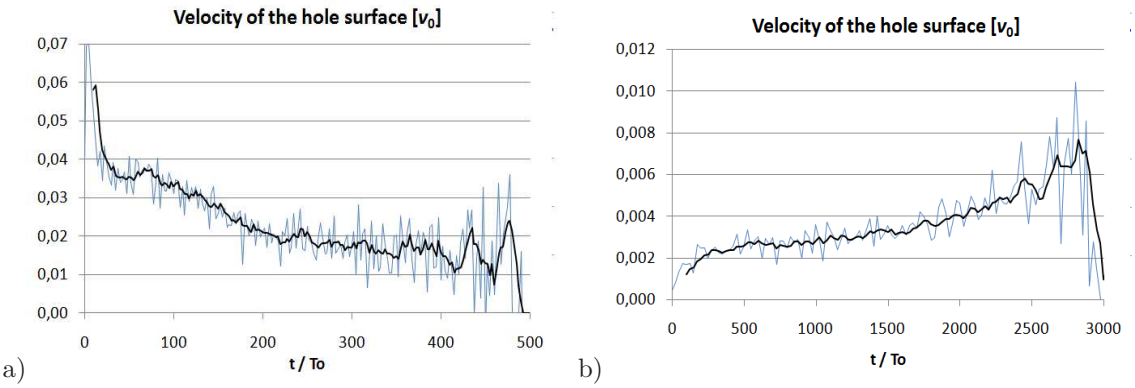

Figure 7: Time dependenceies of the hole surface velocity: a) $r_p = 0.01$, b) $r_p = 0.0002$.

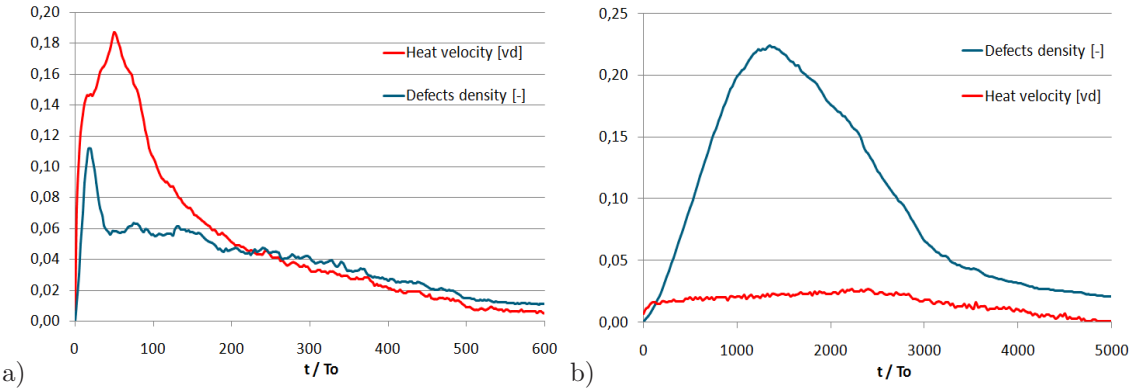

Figure 8: Time dependencies of the heat velocity and relative density of defects: a) $r_p = 0.01$, b) $r_p = 0.0002$.

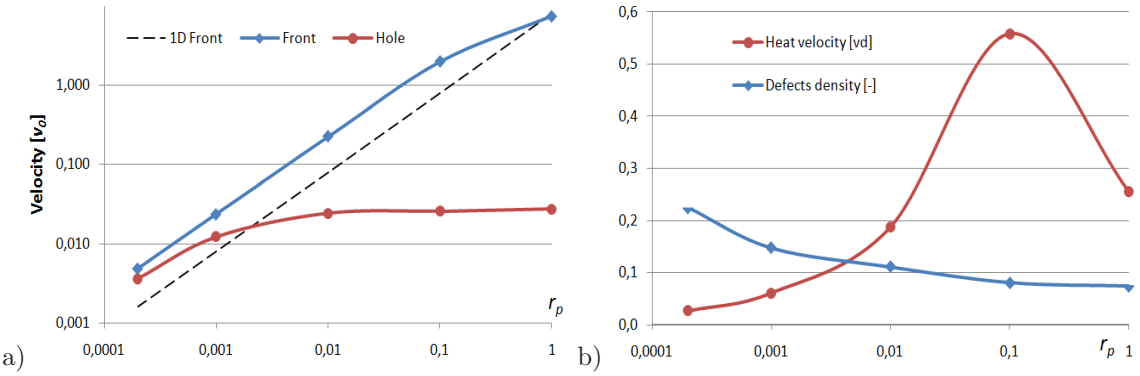

Figure 9: Influence of the reaction probability on: a) chemical front velocity and hole surface velocity; b) heat velocity and relative defects density.

of r_p. However, the lower is r_p, the more time is needed for computation — see Fig. 10. The computation time in the figure is shown as internal time (in units of T_0, left axis) and external time (in minutes, right axis). The external time corresponds to computations on PC with processor Core 2 Duo 2.4 GHz (Sony VAIO VGN-Z21MRN). In the most real situations the front velocity is so low that the corresponding computations would be too long. However the convergence of the results for the lower values of r_p shows that the real situations can be approximated from the realizable computer experiments.

5 Oxidation of circular and square specimens

At the end let us present the computation results where the oxidation starts not from the internal surface, but from the external one. Fig. 11 shows sequential stages of a ball oxidation, Fig. 12 — the same for a square specimen. The ball contains 50 316 particles, the square specimen — 63 920 particles, reaction probability is $r_p = 0.01$, other calculation parameters are same as above. For these experiments the dependencies similar to the above ones can be observed, where instead of the hole surface velocity would act the velocity of the outer surface of the specimen. However the necessary plastic deformations in these cases probably would be lower, then in the case of the internal holes. Indeed, a specimen with an external surface has much better options for relaxation due to export of dislocations and cracks to the surface.

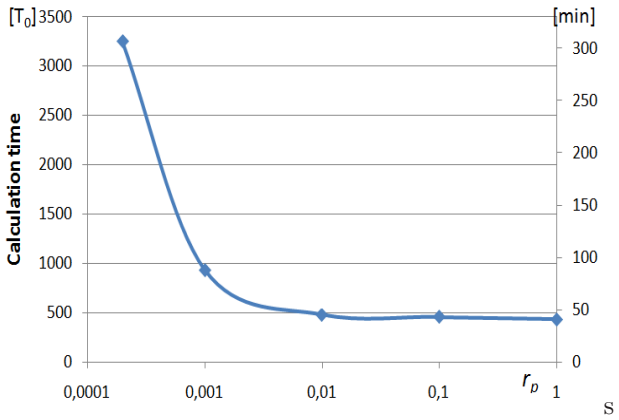

Figure 10: Time of computation as a function of reaction probability r_p.

6 Reaction probability and speed of chemical reaction

In the presented computer experiments it was shown that all parameters of the process depend strongly on the reaction probability r_p and therefore this quantity is very important characteristics for the chemically induced phase transformations and corresponding mechanical processes. The reaction probability has a clear meaning from a computational point of view — it belongs to interval $[0, 1]$ and determines probability of reaction for each particle at each computational step. However, this quantity is not objective from a physical point of view, since the corresponding physical result would depend on the choice of the computational time step Δt. The highest possible value of r_p corresponds to the fastest possible velocity $v_c = a/\Delta t$ of the chemical reaction front propagation. This fastest velocity is pure computational (algorithmic), showing how fast for the current value of time step a computational information can be transferred from one point of the material to another. No physical processes propagating in space faster then v_c can be modelled. However by decrease of Δt this velocity can be set as high as it is needed from the physical point of view. Thus, to characterize the speed of the chemical reaction another physically objective quantity is required. This could be the introduced above velocity v_f of propagation of the chemical reaction front in 1D chain

$$v_f \stackrel{\text{def}}{=} r_p v_c = r_p \frac{a}{\Delta t} = \frac{r_p}{2\pi} \frac{T_0}{\Delta t} v_0. \tag{14}$$

Here v_0 is the sound velocity in 1D chain. To make v_f a physically objective value the ratio $r_p/\Delta t$ should be kept constant with the change of Δt. To do this the required value of r_p can be calculated from formula (14) as

$$r_p = 2\pi \frac{\Delta t}{T_0} \frac{v_f}{v_0}. \tag{15}$$

Another, and, probably, better choice for the quantity characterizing the chemical reaction speed could be

$$\omega_f \stackrel{\text{def}}{=} \frac{r_p}{\Delta t} = \frac{r_p}{2\pi} \frac{T_0}{\Delta t} \omega_0, \tag{16}$$

where $\omega_0 = \sqrt{C/m}$ is an oscillation frequency of a mass m on a string C. Introduce by this way the chemical reaction speed has dimension of frequency, and similarly to (15) the reaction probability should be calculated as

$$r_p = 2\pi \frac{\Delta t}{T_0} \frac{\omega_f}{\omega_0}. \tag{17}$$

In this formula ratio $\Delta t/T_0$ should be set from computational reasons, and ratio ω_f/ω_0 — from physical reasons.

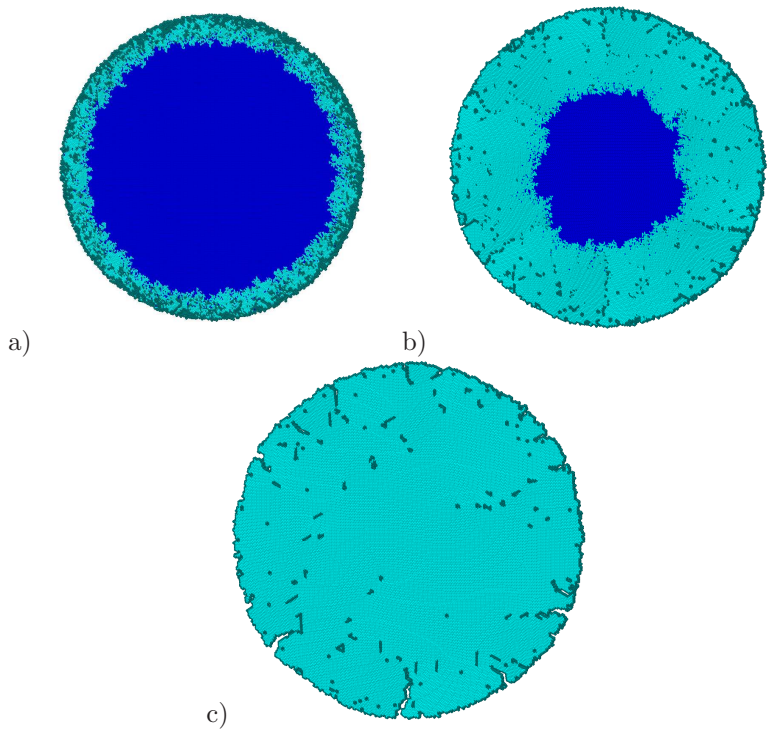

Figure 11: Oxidation of circular specimen: a) $t = 12\,T_0$, b) $t = 40\,T_0$, c) $t = 400\,T_0$.

7 Conclusions

A molecular dynamics model for the phase transformation induced by chemical reaction (oxidation) was presented. It was taken into account that the material properties such as density, stiffness and strength are being changed due to the oxidation. In contrast with the previous stage of the project the oxidation is considered not only on the material surface, but also inside the material at the phase boundaries. To model this phenomenon computational algorithms for the surface and internal oxidation were developed. A reaction probability r_p was introduced to control the speed of the chemical reaction and the velocity of the reaction front. A square specimen with periodic boundaries and central circular hole was considered, which is equivalent to an infinite material with a periodic set of holes. Oxidation starting from the inner surface of the hole and resulting in the hole closure was investigated. Influence of the reaction probability on the velocity of the chemical reaction front, velocity of the hole surface, thermal motion, and defects density were analyzed. In addition oxidation starting from the outer surface of a circular and square specimens was considered.

It was shown that for the high values of the reaction probability the process is dynamical, it is accompanied with a strong thermal effect, the oxidation occurs much faster then mechanical processes such as the hole closure. For the lower values of the reaction probability a quasistatical process with a week thermal effect is realized. In the second case the mechanical processes follow the chemical processes and they have approximately the same speed. This shows that the models for slow chemical processes, which can not be computed directly because of too long time required for such computations, can be extrapolated from the computations with decreasing values of reaction probability. The velocity of the hole surface in the process of the computer experiment is a monotonic function of time, however this function is decreasing for higher reaction probabilities and increasing for lower r_p. As it was mentioned above, the thermal effect of the phase transformation decreases with the decrease of r_p. However this relation has a maximum in the area of the high r_p and it is unexpectedly decreasing when r_p approaches unity. Another unexpected effect is that the density of defects grows with the decrease of the reaction probability. This growth has even accelerative character on the graph with logarithmic r_p-scale — see Fig. 9b. But obviously this

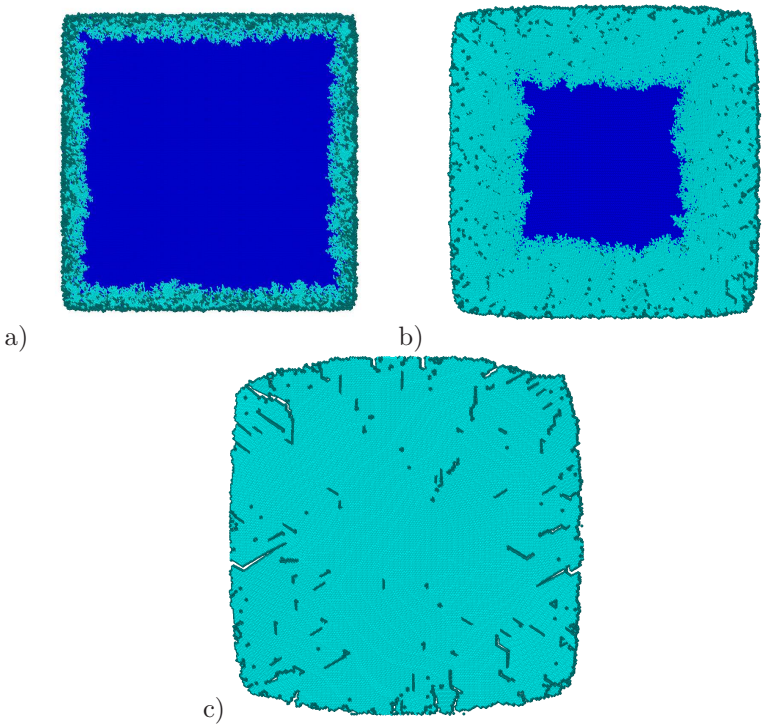

Figure 12: Oxidation of square specimen: a) $t = 12\,T_0$, b) $t = 39\,T_0$, c) $t = 600\,T_0$.

growth can not continue much further since the density of defects can not be too high. Therefore for the lower values of r_p this graph should either tend to a constant value, or should have an extremum (maximum). However these values of r_p were not reached yet due to long computational times, required to perform such calculation.

The listed above questions could be subjects for the further investigations. Besides it would be useful to extend the model of the chemical reaction by modelling the oxygen transfer through the oxide and applying thermodynamic conditions at the reaction front.

Acknowledgements

This work was supported by Sandia National Laboratories and RFBR grants 08-01-00865-a and 09-01-12096-ofi-m. The author is grateful to A. B. Freidin and E. N. Vilchevskaya for the useful discussions.

References

[1] C. L. Muhlstein, S. B. Brown, and R. O. Ritchie. High-cycle Fatigue and Durability of Polycrystalline Silicon Thin Films in Ambient Air. Sensors and Actuators, A 94. Elsevier, pp.177-188 (2001).

[2] A. M. Krivtsov. Influence of defects type and chemical reaction on fracture initiation, molecular dynamics study. Proc. for the Joint U.S. and Russia Conference on Advances in Materials Science. Prague, 2009.

[3] A. M. Krivtsov. MD modeling of low-cycle high-amplitude loading of monocrystal material with defects. Proc. of XXXIII Summer School “Advanced Problems in Mechanics 2005”, St. Petersburg, Russia, 2006, 341-346.

[4] A. M. Krivtsov. Molecular dynamics simulation of plastic effects upon spalling. Phys. Solid State **46**, 6 (2004).

[5] M. P. Allen and A. K. Tildesley. Computer Simulation of Liquids. – Oxford: Clarendon Press. 1987. 385.

[6] A. M. Krivtsov. Deformation and fracture of solids with microstructure. Moscow, Fismatlit. 2007. 304 p. (In Russian).